Journal of Inflammation Research Dovepress

Open Access Full Text Article ORIGINAL RESEARCH

Menaquinone-4 Alleviates Sepsis-Associated Acute Lung Injury via Activating SIRT3-p53/SLC7A11 Pathway

Nan Gao[1,2], Xiao-Yu Liu[1,2], Jie Chen[1,2], Tian-Peng Hu[1,2], Yu Wang[2,3], Guo-Qiang Zhang[2]

[1]China-Japan Friendship Hospital, Chinese Academy of Medical Sciences and Peking Union Medical College, Beijing, People's Republic of China; [2]Department of Emergency, China-Japan Friendship Hospital, Beijing, 100029, People's Republic of China; [3]Graduate School, Capital Medical University, Beijing, 100069, People's Republic of China

Correspondence: Guo-Qiang Zhang, Department of Emergency, China-Japan Friendship Hospital, Beijing, 10029, People's Republic of China, Tel +8613701054849, Email zhangchong2003@vip.sina.com

Background: Sepsis-associated acute lung injury (SI-ALI) is triggered by various direct or indirect noncardiogenic factors affecting the alveolar epithelium and capillary endothelial cells. Menaquinone-4 (MK-4), a major component of vitamin K, plays a crucial role as an antioxidant by effectively neutralizing reactive oxygen species (ROS) and safeguarding critical biomolecules from oxidative harm within cells. However, the specific mechanisms and clinical implications of MK-4 in SI-ALI are unclear and require further study.

Methods: Cecal ligation and puncture (CLP) surgery is a commonly used method to induce sepsis in C57BL/6N wild-type mice, and the mice were administered MK-4 at a dosage of 200 mg/kg/day and 3-TYP at 5 mg/kg/day via intraperitoneal injection for 3 days, or erastin (5 mg/kg) 0.5 hours before CLP surgery. The mice were sacrificed 24 hours after CLP surgery, and blood and lung tissue samples were collected. Pathological changes in the lung tissue and oxidative stress levels were detected. The expression levels of Sirt3, acetylated lysine, p53, SLC7A11 ALOX12 and ferroptosis-related proteins were determined. ligation and puncture (CLP)

Results: In this study, we observed that the lung inflammation was associated with reduced Sirt3 expression and increased acetylated lysine levels. The progression of SI-ALI was mitigated by MK-4 through its role in upregulating Sirt3 expression. MK-4 achieved antioxidant effects by downregulating ROS and inflammatory factor levels. Mechanistically, MK-4 inhibited the p53/SLC7A11 signalling pathway in ferroptosis by inhibiting the acetylation of p53, independent of p53 levels. In addition, MK-4 inhibited ferroptosis independent of GPX4. These findings indicate that MK-4 is a promising novel therapeutic agent for treating SI-ALI and possibly sepsis.

Conclusion: These experiments revealed that MK-4 acts as a ferroptosis suppressor, increasing the expression of Sirt3, inhibiting the p53/SLC7A11 signalling pathway, and reducing oxidative stress and inflammatory responses, thereby exerting a protective effect against ALI in sepsis.

Keywords: MK-4, Sirt3, acetylation, p53, ferroptosis, SI-ALI

Introduction

Acute lung injury (ALI) is one of the most common complications in sepsis patients, often arising early in the disease course.[1] A multitude of factors collectively contribute to the development of sepsis-associated ALI (SI-ALI), which is currently thought to be associated with the dysregulated activation of immune cells and aberrant release of mediators.[2,3] Despite years of research and ongoing randomized controlled trials, a targeted treatment capable of saving lives among individuals with sepsis is still lacking.

Acute and chronic cellular stress, stemming from abnormal metabolic and biochemical processes, can initiate a pervasive form of non-apoptotic cell death known as ferroptosis.[4] Ferroptosis is driven by iron-dependent phospholipid peroxidation.[5] Owing to the high polyunsaturated fatty acid (PUFA) content, oxygen free radicals (reactive oxygen species, ROS) attack phospholipid molecules on the surface of the cell membranes and organelle membrane and shorten the life span of cells.[6] In sepsis, the overproduction of ROS triggers a persistent systemic inflammatory response.[7,8] Mitochondria are the main source

Received: 24 August 2024
Accepted: 15 October 2024
Published: 24 October 2024

of ROS in the body. Studies have shown that Sirt3 can be quickly deacetylated in mitochondria in response to mitochondrial stress. The overexpression of Sirt3 can inhibit the ability of the acetylated transcription factors to regulate the mitochondrial glycolytic pathway and tricarboxylic acid cycle.[9] Sirt3 overexpression can also directly neutralize manganese superoxide dismutase (Mn-SOD2) and other enzymes that catalyse the conversion of superoxide to water and hydrogen peroxide to reduce mitochondrial oxidative stress.[10] p53 is a tumour suppressor protein crucial for the DNA damage response and regulation of the cell cycle. In addition to its role in tumour suppression, p53 is also involved in the cellular response to oxidative stress.[11] Sirt3 is a novel suppressor of p53-mediated ferroptosis, and inactivation of Sirt3 significantly increases the sensitivity of cells to p53-dependent ferroptosis under ROS-induced stress.[12]

Menaquinone-4 (MK-4) is sourced primarily from foods such as meat, egg yolk, and dairy products. It can also be synthesized in the body through the conversion of vitamins K1 and K2.[13] MK-4 is known for its roles in bone metabolism and blood coagulation and its anti-inflammatory properties, and is extensively utilized for preventing osteoporosis and enhancing coagulation.[14,15] Moreover, as its anti-inflammatory effects have been further elucidated, MK-4 has been applied to address a range of inflammatory and oxidative stress conditions in the body, including tumours, cognitive disorders, and infections.[16–18] As early as 2010, nutritionists reported that the dietary intake of MK-4 was associated with a reduced risk of fatal cancers.[19] Before the concept of ferroptosis emerged, the antioxidant effects of MK-4 were documented, although the underlying mechanism remained unclear.[20] In 2022, researchers reported the inhibitory effect of MK-4 on ferroptosis.[21] Subsequent investigations revealed the anti-inflammatory role of MK-4 in the circulation during ischaemia-reperfusion, confirming the protective effect of MK-4.[22] In addition, studies revealed that p53 activated ferroptosis and tumour inhibition by regulating MK-4 metabolism, which is beneficial for the treatment of COVID-19.[23,24] The purpose of this study was to explore the protective effects of MK-4 against SI-ALI and its potential mechanisms.

Materials and Methods

Animals

The male C57BL/6N mice were obtained from Beijing Vital River Laboratory Animal Technology Co., Ltd. (Beijing, certificate no. SCXK 2021–0011). The animal experiments were approved by the Animal Ethics Committee of the China-Japan Friendship Institute of Clinical Medical Sciences (ZRDWLL230044). All the experimental procedures were performed following the Guidelines for the Care and Use of Laboratory Animals formulated by the Ministry of Science and Technology of the People's Republic of China. Standard specific pathogen-free conditions were maintained for the mice, which had unrestricted access to water and food in their housing.

Animal Models and Treatment

Male C57BL/6N mice weighing 20–22 g and aged 6–8 weeks were randomly assigned to the experimental groups. Prior to the procedure, the mice were fasted for 12 hours and allowed to drink water normally. Continuous anaesthesia was achieved via inhalation of 1.5% isoflurane. A 1~2 cm longitudinal incision was made along the midline of the abdomen 1 cm below the xiphoid process, and the caecum was exteriorized and ligated with 6–0 silk at half of its length. The intestinal wall was perforated twice with a 7-gauge needle at the midpoint between the distal end and the ligation point. Gentle pressure was applied to the intestinal tube to release an appropriate amount of the intestinal contents, after which the caecum was returned to the abdominal cavity. The layers of the abdomen were closed, and the incision was disinfected. To prevent dehydration, all mice received a subcutaneous injection of sterile isotonic sodium chloride solution at a rate of 5 mL per 100 g of body weight.

Male C57BL/6N mice were randomly divided into 6 groups: the control group, sepsis group (CLP group), menaquinone-4 group (MK-4 group), sepsis + menaquinone-4 group (CLP + MK-4 group), sepsis + menaquinone-4 + Sirt3 inhibitor group (CLP + MK-4 + 3-TYP group), and sepsis + menaquinone-4 + ferroptosis promoter group (CLP + MK-4 + erastin group). Septic mice were established via the CLP method as described previously[25] Before CLP surgery, the mice were administered MK-4 (200 mg/kg/day, HY-B2156, MedChemExpress, China) or 3-TYP (5 mg/kg/day, HY-108331, MedChemExpress, China) by intraperitoneal injection for 3 days and erastin (5 mg/kg, HY-15763, MedChemExpress, China) 0.5 hour before the surgery. The mice were sacrificed 24 hours after CLP, and blood and lung tissue samples were collected.

Western Blot Analysis

Lung tissues from the mice were subjected to Western blotting. The lung tissues were homogenized via ultrasonication and lysed in radioimmunoprecipitation assay (RIPA) lysis buffer (Cat# PC101; EpiZyme Biotechnology, China) containing 1× protease inhibitor cocktail (Cat# P1265; 1:100; Applygen, China) and 1× deacetylase inhibitor cocktail (K0030; 1:100; MedChemExpress, China). Total protein was extracted, and the protein concentration was measured using a BCA protein assay kit (Cat# 23225; Thermo Fisher Scientific, China). After the proteins were separated by electrophoresis on a 10% sodium dodecyl sulfate (SDS)–polyacrylamide gel (Cat# PG213; EpiZyme Biotechnology, China), the proteins were transferred to polyvinylidene fluoride (PVDF) membranes, which were blocked with QuickBlock™ blocking buffer (Cat# 37515; Thermo Fisher Scientific, China) for 10 minutes. The PVDF membranes were incubated with primary antibodies (anti-Sirt3 (D22A3; 1:1000, Cell Signaling Technology, USA), anti-p53 (#ab26; 1:1000, Abcam, USA), anti-SLC7A11 (ab275411; 1:1000, Abcam, USA), anti-acetylated lysine (#9441; 1:1000, Cell Signaling Technology, USA), anti-GPX4 (ab125066; 1:1000, Abcam, USA), anti-ferritin (ab75973; 1:1000, Abcam, USA), anti-ALOX12 (ab211506; 1:1000, Abcam, USA) and anti-GAPDH (Cat# HRP-60004; 1:1000, Proteintech, China)) overnight at 4 °C. After being washed, HRP-labelled goat anti-mouse (Cat# SA00001-1; Proteintech, China) or anti-rabbit (Cat# ZB-2301; 1:10000, ZSGB-BIO, China) secondary antibodies were applied for 1 h at room temperature. The band intensities were quantified via ImageJ software and normalized to the level of GAPDH. For better representation, the expression values in the sham or control group were further adjusted to 1 on the basis of the mean value.

Total RNA Extraction and Absolute RNA Quantification by qPCR

Total RNAs were extracted from mouse lung tissue using the RNA Extraction kit (Cat# AG21024; Accurate Biology, China) according to the instructions. RNA was reversely transcribed to cDNA templates using EVO M-MLVRT Reaction Mix Kit with gDNA Clean for qPCR Ver.2 (Cat# AG11728; Accurate Biology, China) and amplified. Semiquantitative polymerase chain reaction (PCR) was performed using BrightCycle Universal SYBR Green qPCR mix with UDG (Cat# 21219; ABclonal, China) and QuantStudio 5 qPCR Platform (Applied Biosystems) with following the cycle conditions: 37°C for 2min, 95°C for 3 min; 40 cycles of denaturation at 95°C for 5s; annealing and amplification at 65°C for 30s. qPCR primers were as follows: Sirt3 F: 5# GCTTCTGCGGCTCTATACACA 3# R: 5# GTGGGCTTCAACCAGCTTTG 3#; p53 F: 5# TGAGGTTCGTGTTTGTGCCT 3# R: 5# GCAGTTCAGGGCAAAGGACT 3#; SLC7A11 F: 5# AGTC CCGATCTTTGTTGCCC 3# R: 5# CCGGAGAAGAGCATCACCAT 3#.

ELISA

Whole blood from mouse hearts was immediately incubated at 37°C for 15 minutes, and then centrifuged at 3000 rpm for 10 minutes, after which the serum was separated. The expression levels of IL-6 and TNF-α were subsequently measured following the instructions provided with the ELISA kit (GEM0001-48T; GEM0004-48T, Servicebio, China), with three replicates per group.

Immunofluorescence Staining

The frozen sections were rewarmed at room temperature while moisture was controlled. A self-fluorescence quencher was then added, and the tissues were incubated for 5 minutes and then rinsed with water for 10 minutes. Next, an ROS dye solution (D7008; 1:500, Sigma, Germany) was applied to the circled areas on the sections, and the slides were incubated at 37°C in a dark incubator for 30 minutes. The slides were placed in PBS (pH 7.4) (G0002; Servicebio, China) and shaken on a decolorizing shaker for 3 cycles, with each cycle lasting 5 minutes. To stain the nuclei, a DAPI dye solution (G1012; Servicebio, China) was added to the slides, and the slides were incubated at room temperature in the dark for 10 minutes. The slides were subsequently placed again in PBS (pH 7.4) and shaken on a decolorizing table for 3 cycles, each lasting 5 minutes, to remove any excess DAPI dye. Finally, the slides were sealed with anti-fluorescence quenching sealing solution (G1401; Servicebio, China). DAPI fluorescence was detected at an excitation wavelength of 488 nm (range: 465–495 nm) and emission wavelengths between 515 and 555 nm, whereas CY3 fluorescence was detected at an excitation wavelength of 510–560 nm and an emission wavelength of 590 nm.

Immunohistochemical Staining

For histological assessment of acute lung injury, mouse lung sections were subjected to immunohistochemical staining. The tissue sections were first sealed with 3% H2O2 and incubated in 10% goat serum for 1 hour. Subsequently, primary antibodies were applied, and the samples were incubated overnight at 4°C. Next, secondary antibodies were applied, and the slides were counterstained with Harris haematoxylin and mounted with a neutral adhesive. Imaging was performed using a Leica microscope (Leica Microsystems, Germany), and the collected images were analysed.

Co-Immunoprecipitation Assays

Lung tissues were collected from each group and then homogenized in NP-40 IP lysis buffer (Cat# RM00022; ABclonal, China) supplemented with protease and deacetylase inhibitors. The homogenized samples were subsequently centrifuged at 14,000 × g for 5 minutes at 4°C. The supernatants were collected and incubated with the indicated primary antibody overnight at 4°C. Protein A+G magnetic beads (#73778S; Cell Signaling Technology, USA) that were preequilibrated in lysis buffer were added to the samples. The following primary antibodies were used for IP: anti-Sirt3 (D22A3; 1:500; Cell Signaling Technology, USA), anti-p53 (#ab26; 1:500; Abcam, USA), and anti-acetylated lysine (#9441; 1:1000; Cell Signaling Technology, USA). The beads were collected by centrifugation at 3000 × g for 5 minutes, washed, and then resuspended in an equal volume of 5x SDS loading buffer. Next, the complexes were analysed by Western blotting, and total protein was used as the input in the analysis.

Histology

Histological analysis of mouse lung tissues was performed via haematoxylin and eosin (HE) staining. Fresh lung tissues were sliced into sections, fixed in 10% formalin for approximately 24 hours, stained and observed under an optical microscope. The lung injury score was assessed based on an Official American Thoracic Society Workshop Report: Features and Measurements of Experimental Acute Lung Injury in Animals.[26,27]

Survival Study

Thirty-six mice were randomly divided into three groups. One group received a daily intraperitoneal injection of MK-4 for 3 days, with the last injection given 1 hour before CLP. One group received an equivalent volume of saline solution before CLP. The other group received an equivalent volume of saline solution before sham surgery. The mice were observed for 3 days (72 hours) from the end of the modelling procedure. The average survival rate and survival time were calculated.

Statistical Analysis

Data analysis was conducted with GraphPad Prism 9 (San Diego, CA, USA). The results are presented as the mean ± standard error of the mean (SEM). The data were first tested for normality and equality of variance. Student's *t*-test or the Mann–Whitney test (unequal variance or nonnormal distribution) was used for comparisons between two groups. ANOVA followed by Tukey's post hoc test was used to analyse differences among multiple groups. The data are presented as the means ± SEMs. $P<0.05$ was considered to indicate a statistically significant difference.

Results

Changes in the Sirt3/p53/SLC7A11 Signalling Pathway in SI-ALI

To investigate the role of Sirt3 in SI-ALI, we first dynamically observed the gross model of ALI. As shown in Figure 1A and B), we observed an increase in the destruction of the alveolar structure, resulting in significant septal oedema, alveolar exudation, and congestion in a time-dependent manner, indicating increased lung injury during the development of sepsis. As shown in Figure 1C and D), the expression of Sirt3 obviously decreased after 6 hours, whereas the acetylated-lysine level in whole lung tissue increased (Figure 1G and H). In the p53/SLC7A11 signalling pathway, as shown in Figure 1C, E and F), SLC7A11 protein expression decreased in a time-dependent manner, whereas p53 expression remained unchanged. However, compared with those in the sham group, the binding of p53 and Sirt3 in the lung tissue of mice 24 hours after CLP was significantly decreased

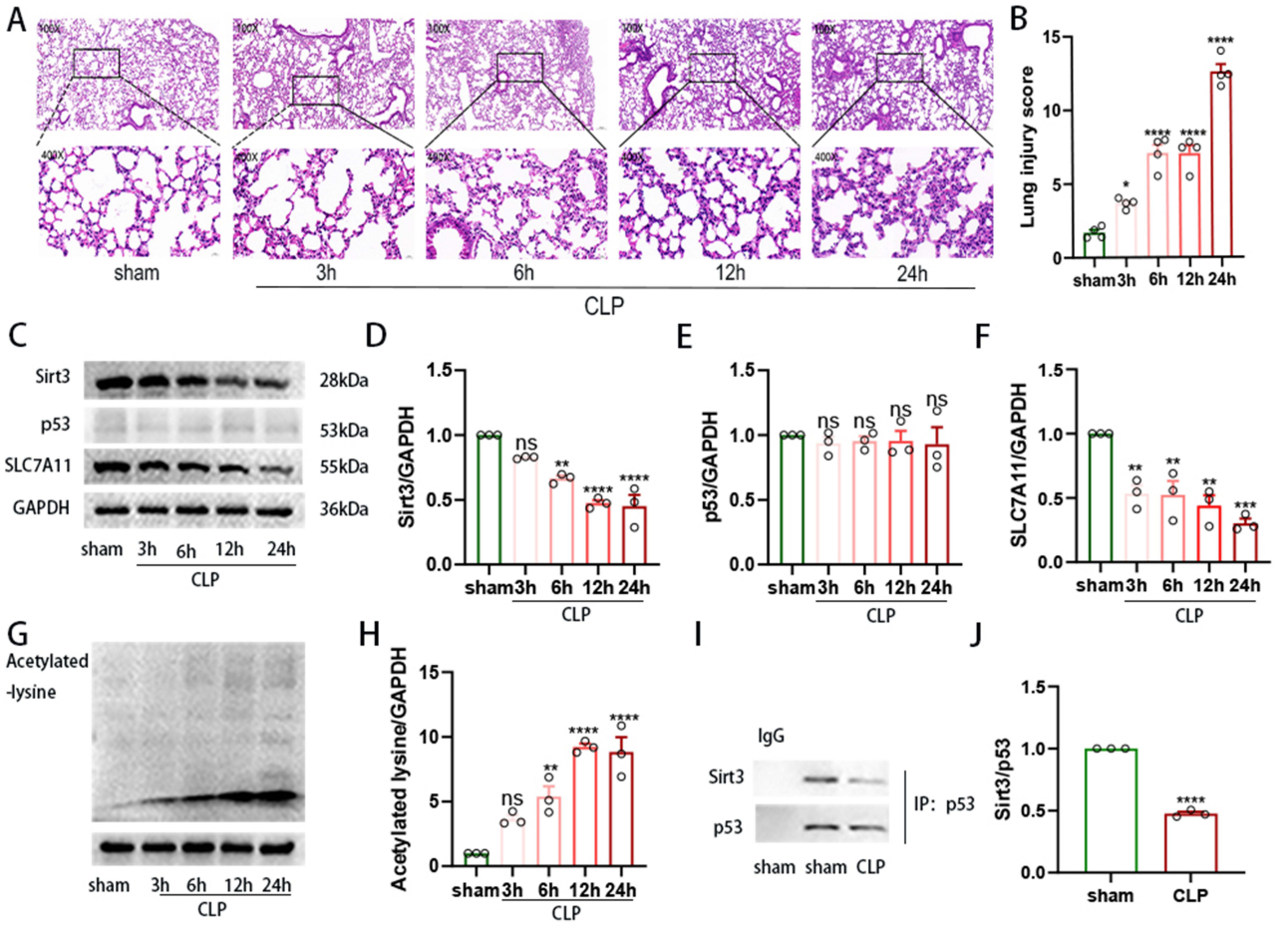

Figure 1 The downregulation of Sirt3 was accompanied by increased inflammation in an ALI model. (**A**). HE staining of lung tissues from CLP-induced ALI model mice at different time points. Magnification: ×200 and ×400. (**B**) Lung injury score. (**C–H**). Quantification of the relative expression of Sirt3, SLC7A11, p53 and acetylated lysine in the CLP-induced ALI mouse model (n=3). (**I-J**). The capacity of Sirt3 to bind to p53 was assessed by IP analysis (n=3). "*" indicates a significant difference between the corresponding groups (*p < 0.05, **p < 0.01, ***p < 0.001, ****p < 0.0001).

(Figure 1I and J). Therefore, our results indicated that the p53/SLC7A11 signalling pathway participated in SI-ALI in a Sirt3-dependent-deacetylation manner.

MK-4 Inhibits Oxidative Stress and Inflammation in SI-ALI

To investigate the regulation of oxidative stress by MK-4 in SI-ALI, we employed immunofluorescence to observe ROS. As shown in Figure 2A and B), compared with those in the control group or the sham group, the ROS levels in the CLP group were significantly increased. However, the level of ROS was notably lower in the MK-4 + CLP group than in the CLP group, which indicated that MK-4 ameliorated oxidative stress in SI-ALI. ELISAs were subsequently used to measure the levels of IL-6 and TNF-α in the different groups. As shown in Figure 2C and D), compared with those in the control group, the levels of IL-6 and TNF-α were significantly elevated in the CLP group. However, in the serum of the CLP + MK-4 group, the levels of these two inflammatory factors were notably lower than those in the CLP group. These findings demonstrated that MK-4 reduced the levels of inflammatory cytokines in SI-ALI.

MK-4 Ameliorates SI-ALI by Promoting Sirt3 Expression

Previous studies have shown that MK-4 can effectively inhibit ferroptosis in models, including ferroptosis induced by GPX4 inhibitor treatment, GPX4 knockout, cystine starvation and glutamine treatment.[23] To compare the effects of MK-4 and Sirt3, we treated septic mice with MK-4 and 3-TYP. As shown in Figure 3A–F), the expression of Sirt3, p53, SLC7A11 and total acetylated lysine in the lung tissues of the MK-4 group did not exhibit significantly differ from that in

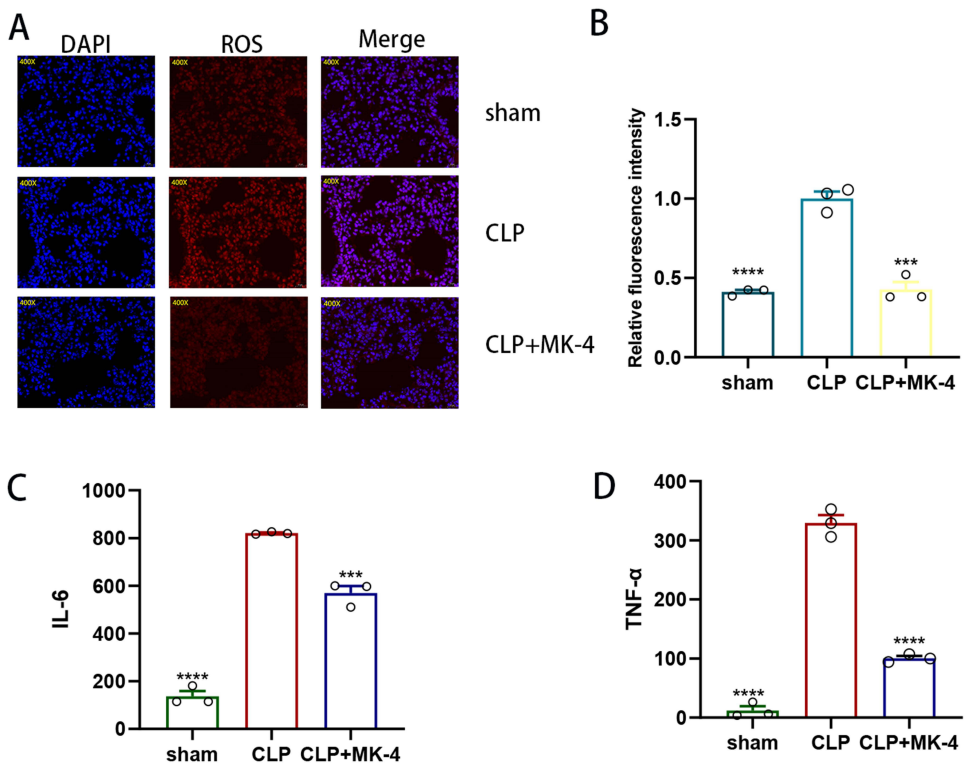

Figure 2 MK-4 protects against SI-ALI by ameliorating oxidative stress and inflammatory responses. (**A** and **B**) Immunofluorescence staining and quantitative detection of ROS levels in lung tissue. Magnification: ×200 (n=3). (**C** and **D**) ELISA was used to measure the levels of IL-6 and TNF-α in cardiac blood (n=3). The data are presented as the means ± SEMs. "*" indicates a significant difference between the corresponding groups (***p < 0.001, ****p < 0.0001).

the control group. Compared with that in the control group, the expression of Sirt3 was significantly decreased in the CLP group, whereas the level of acetylated lysine was significantly increased. However, compared with that in the CLP group, the expression of Sirt3 was significantly increased, whereas the level of acetylated lysine was decreased in the CLP + MK-4 group. This effect of MK-4 was reversed by 3-TYP. These findings suggest that MK-4 regulates acetylation levels by modulating Sirt3 expression to protect against SI-ALI. In the p53/SLC7A11 signalling pathway, the expression of SLC7A11 in the CLP + MK-4 group was significantly greater than that in the CLP group but lower than that in the control group. Interestingly, the overall expression level of p53, which can inhibit SLC7A11, did not change significantly. However, as depicted by the COIP data in Figure 3G–I), compared with that in the CLP group, the binding of Sirt3 to p53 in the CLP + MK-4 group was greater, accompanied by increased p53 deacetylation. We next examined the mRNA levels of Sirt3, p53 and SLC7A11. As shown in Figure 3J and L), compared with the control group, the mRNA expression of Sirt3 was significantly upregulated, while the mRNA expression of SLC7A11 was significantly increased in the CLP + MK-4 group. However, compared with the control group, the mRNA expression of p53 was downregulated in the CLP +MK-4 group, which was inconsistent with the changes in protein levels in Figure 3K). These results demonstrated that Sirt3 regulated p53 by modulating its acetylation level, independent of the p53 levels.

Ferroptosis Monitoring is Independent of GPX4 and Regulated by MK-4

To confirm the role of MK-4 in ferroptosis, Western blotting was used to measure the expression levels of ferroptosis-related proteins in lung tissues. Compared with those in the control group, the expression levels of Sirt3, SLC7A11, ALOX12, and ferritin were significantly lower in the CLP group as shown in Figure 4A–F). However, compared with those in the CLP group, the increase in Sirt3 levels paralleled the increasing in ALOX12 and ferritin protein levels in the CLP + MK-4 group. In addition, the expression of ALOX12 and ferritin in lung tissues from the MK-4- and erastin-induced CLP groups was significantly lower than that in lung tissues from the control group and the MK-4 + CLP group (Figure 4A, D–F). However, as shown in Figure 4G-H, I, K), Western blotting and immunohistochemistry revealed no

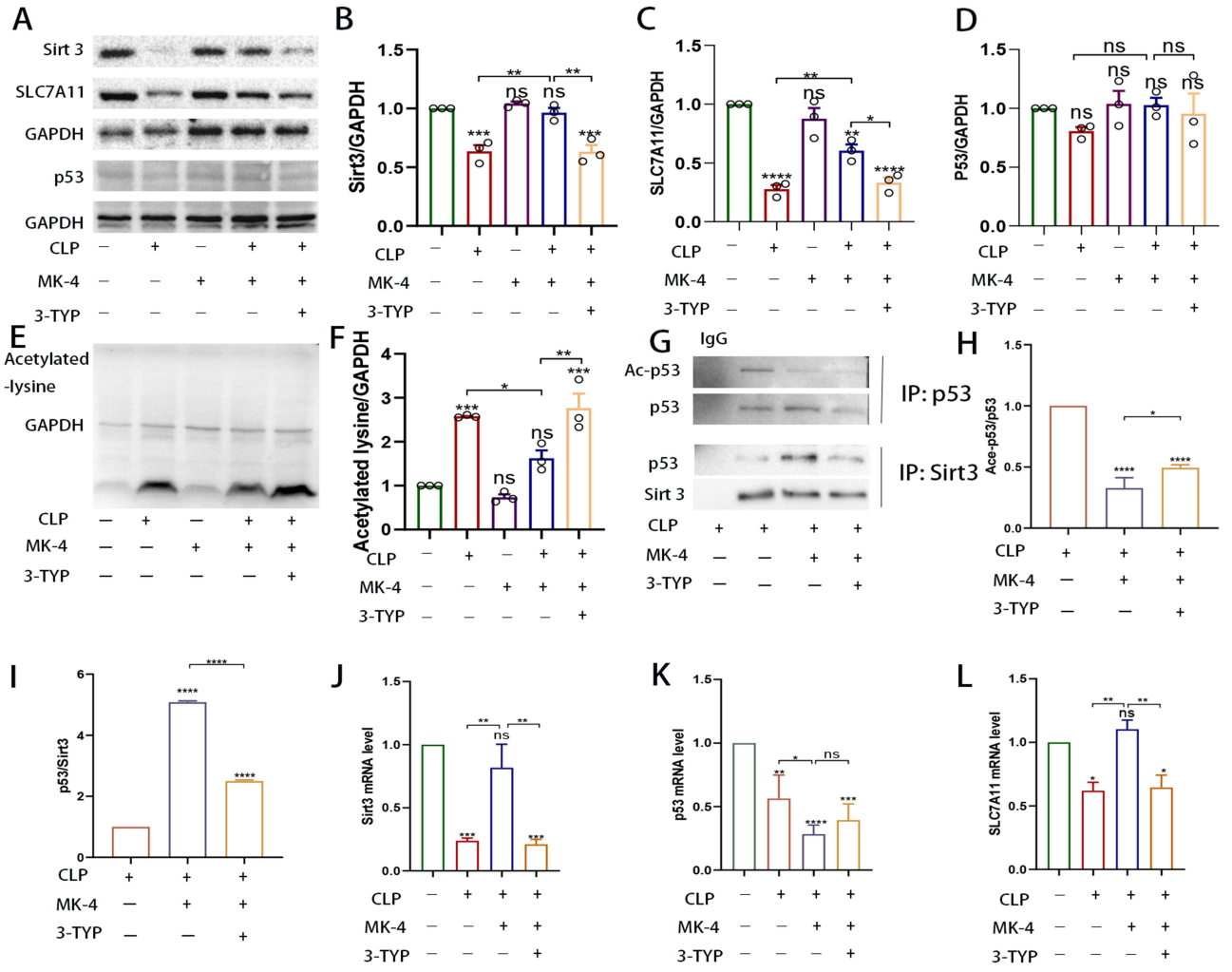

Figure 3 MK-4 promoted the expression of the Sirt3 and alleviated the acetylation of p53 induced by CLP. (**A–F**) Quantification of the relative expression of Sirt3, SLC7A11, p53 and acetylated lysine. (**G–I**) The acetylation of p53 and the ability of Sirt3 to bind to p53 were assessed by IP analysis. (**J–L**) The mRNA level of Sirt3, p53 and SLC7A11 in lung tissues of CLP-induced ALI. "*" indicates a significant difference between the corresponding groups (*p < 0.05, **p < 0.01, ***p < 0.001, ****p < 0.0001).

significant changes in the expression of GPX4 among the groups, which was consistent with previous studies.[23,28] These results suggested that MK-4 inhibited ferroptosis via p53/SLC7A11/ALOX12-independent pathway by modulating Sirt3, independent of the classical GPX4 pathway. As shown in Figure 4I and J), compared with HE staining in the CLP group, The severity of lung tissue injury was significantly alleviated in the CLP + MK-4 group; however, this effect of MK-4 was reversed by erastin. Notably, treatment with the ferroptosis promoter inhibitor erastin significantly increased lung injury score in SI-ALI, indicating that MK-4 inhibited the occurrence of ferroptosis.

MK-4 Improved the Survival Rate of Mice with Sepsis

We observed and recorded the 72-hour survival time of the mice in the sham group, CLP group and CLP + MK-4 group. As shown in Figure 5, compared with the CLP group, the CLP group treated with MK-4 presented a slightly delayed earliest time of death and the 3-day survival rate was obviously improved. The therapeutic effect of MK-4 on septic mice significantly outweighed any potential harm, and this difference was statistically significant (p = 0.0065).

Discussion

In sepsis, the immune system is overactivated and initiates an excessive inflammatory response, resulting in a "cytokine storm". This cytokine storm causes widespread tissue damage, organ dysfunction, and even multiple organ failure if not

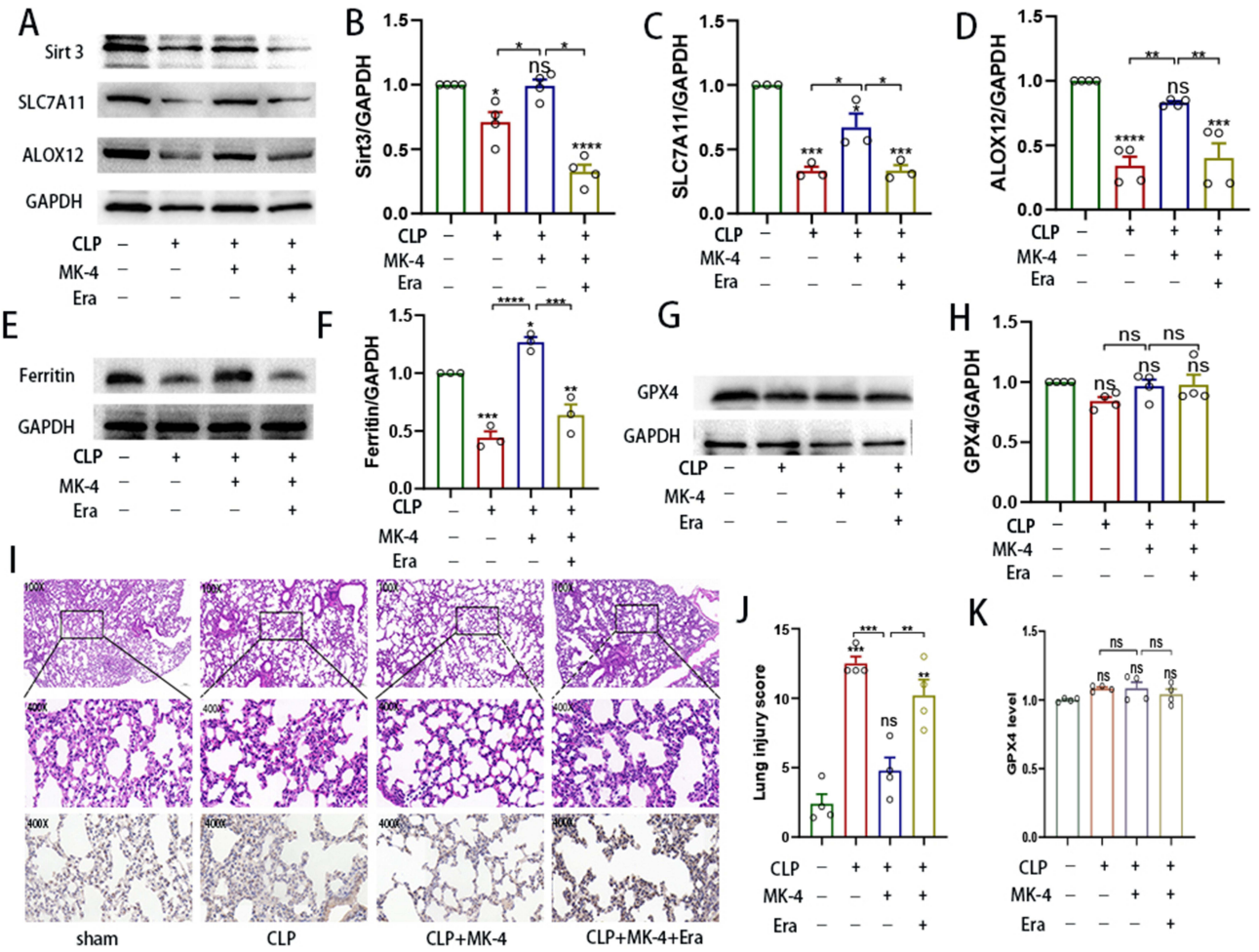

Figure 4 MK-4 is a ferroptosis inhibitor. (**A**–**H**) Western blot analysis of Sirt3, SLC7A11, ALOX12 and ferroptosis-related expression in SI-ALI. (**I**). Histology and immunohistochemical analysis of GPX4 levels in the different groups. Magnification: ×200 and ×400. (**J**) Lung injury score. (**K**) Quantification of the relative expression of GPX4. "*" indicates a significant difference between the corresponding groups (*p < 0.05, **p < 0.01, ***p < 0.001, ****p < 0.0001).

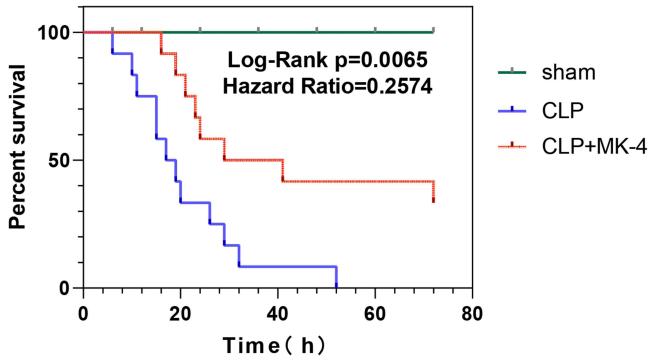

Figure 5 Effect of MK-4 on survival rate of septic mice. The green line represents the sham group, the red line indicates the CLP group treated with MK-4, and the blue line denotes the CLP group (n=12).

properly managed.[29] Considerable evidence suggests that Sirt3 plays a protective role in the pathogenesis of sepsis. Sirt3 serves as an NAD-dependent protein deacetylase within mitochondria. Its role in regulating mitochondrial oxidative stress, apoptosis, and metabolism is crucial for maintaining cellular integrity and function.[9,30,31] Sirt3 has been found to act as an inhibitor of the inflammatory response in sepsis through various mechanisms, regulated oxidative stress and

protecting mitochondrial function and the intracellular metabolic balance.[32,33] The expression of Sirt3 is inhibited in sepsis, which leads to mitochondrial dysfunction, intensifying cellular oxidative stress and the inflammatory response.[34] In the present study, we found that in SI-ALI, the expression of Sirt3 decreased in a time-dependent manner and this decrease was accompanied by increased global acetylated lysine levels. Pharmacological inhibition of Sirt3 by 3-TYP treatment significantly increased global acetylation levels in vivo. These results highlight the importance of the deacetylation effects of Sirt3 in ALI, which is consistent with previous study.[35]

Previous studies have shown that the regulatory effect of Sirt3 on p53 involves the modulation of its acetylation, which is independent of the levels of p53 and p53-mediated transcriptional activity.[12,36,37] MK-4 plays a crucial role in the coagulation process by helping the blood clot properly. This is important for preventing excessive bleeding and maintaining normal coagulation function.[38,39] MK-4 can also act as an antioxidant by neutralizing free radicals and reducing oxidative damage.[40] In this study, we demonstrated that MK-4 achieved antioxidant effects by reducing ROS levels in SI-ALI. With respect to oxidative stress, we found that septic mice treated with MK-4 presented an obvious decrease in the levels of common inflammatory factors and an improvement in inflammatory cell infiltration in lung tissue.

In addition, we demonstrated the remarkable ability of MK-4 to inhibit ferroptosis by reducing the expression of Sirt3, which ultimately improved mortality in mice with sepsis. Accumulating evidence indicates that p53 promotes ferroptosis by regulating SLC7A11 in both GSH-dependent and GSH-independent manners.[28,41] Erastin is a drug that induces ferroptosis by either suppressing the intrinsic antioxidant system of the cell or increasing its susceptibility to oxidative stress. In this study, we found that MK-4 increased the levels of ferritin and ALOX12, proteins associated with ferroptosis, but did not affect GPX4 expression. These findings suggest that MK-4 regulates ferroptosis independently of the classical GPX4 pathway. These results indicate that MK-4 shows promise as a potential therapy for sepsis. Several preliminary studies have suggested that MK-4 injection in patients with sepsis may help to balance the coagulation system by improving anticoagulant activity.[42] However, more studies are needed to verify the safety and efficacy of this treatment. p53 is a crucial tumor suppressor protein, characterized by a complex regulatory network that enables cells to respond appropriately to a wide range of physiological and pathological conditions, the role of p53 in acute lung injury during sepsis requires further investigation. In summary, while MK-4 has shown potential in suppressing sepsis by targeting Sirt3, additional intensive studies and clinical trials are needed to fully evaluate its effectiveness and determine the precise mechanisms underlying its therapeutic effect. These findings will ultimately provide more specific and effective treatment approaches for sepsis management.

Conclusions

Although the protective role of Sirt3 in inflammatory responses is known, its specific protective function in sepsis remains unclear, and there is a lack of effective regulatory drugs. MK-4 can serve as an inhibitor of ferroptosis and modulate the expression of Sirt3. It not only improves sepsis-associated acute lung injury by regulating the p53/SLC7A11 signaling pathway but also alleviates oxidative stress and inflammation levels in SI-ALI. These results offer new perspectives for identifying novel targets to treat sepsis.

Funding

This work was supported by the National High Level Hospital Clinical Research Funding of China (2022-NHLHCRF-YS-03) and the National Natural Science Foundation of China (82272196).

Disclosure

The authors declare that they have no known competing financial interests or personal relationships that could have appeared to influence the work reported in this paper.

References

1. Ware LB, Matthay MA. The acute respiratory distress syndrome. *N Engl J Med*. 2000;342(18):1334–1349. doi:10.1056/NEJM200005043421806
2. Kumar V. Pulmonary innate immune response determines the outcome of inflammation during pneumonia and sepsis-associated acute lung injury. *Front Immunol*. 2020;11:1722. doi:10.3389/fimmu.2020.01722

3. Yang HH, Duan J-X, Liu S-K, et al. A COX-2/sEH dual inhibitor PTUPB alleviates lipopolysaccharide-induced acute lung injury in mice by inhibiting NLRP3 inflammasome activation. *Theranostics*. 2020;10(11):4749–4761. doi:10.7150/thno.43108
4. Zheng J, Conrad M. The metabolic underpinnings of ferroptosis. *Cell Metab*. 2020;32(6):920–937. doi:10.1016/j.cmet.2020.10.011
5. Liang D, Minikes AM, Jiang X. Ferroptosis at the intersection of lipid metabolism and cellular signaling. *Mol Cell*. 2022;82(12):2215–2227. doi:10.1016/j.molcel.2022.03.022
6. Yang WS, Kim KJ, Gaschler MM, et al. Peroxidation of polyunsaturated fatty acids by lipoxygenases drives ferroptosis. *Proc Natl Acad Sci U S A*. 2016;113(34):E4966–75. doi:10.1073/pnas.1603244113
7. Patoli D, Mignotte F, Deckert V, et al. Inhibition of mitophagy drives macrophage activation and antibacterial defense during sepsis. *J Clin Invest*. 2020;130(11):5858–5874. doi:10.1172/JCI130996
8. Liu C, Zou Q, Tang H, et al. Melanin nanoparticles alleviate sepsis-induced myocardial injury by suppressing ferroptosis and inflammation. *Bioact Mater*. 2023;24:313–321.
9. Xu Y, Zhang S, Rong J, et al. Sirt3 is a novel target to treat sepsis induced myocardial dysfunction by acetylated modulation of critical enzymes within cardiac tricarboxylic acid cycle. *Pharmacol Res*. 2020;159:104887. doi:10.1016/j.phrs.2020.104887
10. Dikalova AE, Itani HA, Nazarewicz RR, et al. Sirt3 Impairment and SOD2 hyperacetylation in vascular oxidative stress and hypertension. *Circ Res*. 2017;121(5):564–574. doi:10.1161/CIRCRESAHA.117.310933
11. Yang Y, White E. Autophagy suppresses TRP53/p53 and oxidative stress to enable mammalian survival. *Autophagy*. 2020;16(7):1355–1357. doi:10.1080/15548627.2020.1765522
12. Jin Y, Gu W, Chen W. Sirt3 is critical for p53-mediated ferroptosis upon ROS-induced stress. *J Mol Cell Biol*. 2021;13(2):151–154. doi:10.1093/jmcb/mjaa074
13. Chatron N, Hammed A, Benoît E, et al. Structural Insights into Phylloquinone (Vitamin K1), Menaquinone (MK4, MK7), and Menadione (Vitamin K3) Binding to VKORC1. *Nutrients*. 2019;11(1):67. doi:10.3390/nu11010067
14. Rannels SR, Gallaher KJ, Wallin R, et al. Vitamin K-dependent carboxylation of pulmonary surfactant-associated proteins. *Proc Natl Acad Sci U S A*. 1987;84(16):5952–5956. doi:10.1073/pnas.84.16.5952
15. Furie B, Furie BC. Molecular basis of vitamin K-dependent gamma-carboxylation. *Blood*. 1990;75(9):1753–1762. doi:10.1182/blood.V75.9.1753.1753
16. Kaneki M, Hosoi T, Ouchi Y, et al. Pleiotropic actions of vitamin K: protector of bone health and beyond? *Nutrition*. 2006;22(7–8):845–852. doi:10.1016/j.nut.2006.05.003
17. Berkner KL, Runge KW. The physiology of vitamin K nutriture and vitamin K-dependent protein function in atherosclerosis. *J Thromb Haemost*. 2004;2(12):2118–2132. doi:10.1111/j.1538-7836.2004.00968.x
18. Yokoyama T, Miyazawa K, Naito M, et al. Vitamin K2 induces autophagy and apoptosis simultaneously in leukemia cells. *Autophagy*. 2008;4(5):629–640. doi:10.4161/auto.5941
19. Nimptsch K, Rohrmann S, Kaaks R, et al. Dietary vitamin K intake in relation to cancer incidence and mortality: results from the Heidelberg cohort of the European prospective investigation into cancer and nutrition (EPIC-Heidelberg). *Am J Clin Nutr*. 2010;91(5):1348–1358. doi:10.3945/ajcn.2009.28691
20. Westhofen P, Watzka M, Marinova M, et al. Human vitamin K 2,3-epoxide reductase complex subunit 1-like 1 (VKORC1L1) mediates vitamin K-dependent intracellular antioxidant function. *J Biol Chem*. 2011;286(17):15085–15094. doi:10.1074/jbc.M110.210971
21. Mishima E, Ito J, Wu Z, et al. A non-canonical vitamin K cycle is a potent ferroptosis suppressor. *Nature*. 2022;608(7924):778–783. doi:10.1038/s41586-022-05022-3
22. Nakamura T, Hipp C, Santos Dias Mourão A, et al. Phase separation of FSP1 promotes ferroptosis. *Nature*. 2023;619(7969):371–377. doi:10.1038/s41586-023-06255-6
23. Yang X, Wang Z, Zandkarimi F, et al. Regulation of VKORC1L1 is critical for p53-mediated tumor suppression through vitamin K metabolism. *Cell Metab*. 2023;35(8):1474–1490.e8. doi:10.1016/j.cmet.2023.06.014
24. Nuszkiewicz J, Sutkowy P, Wróblewski M, et al. Links between Vitamin K, Ferroptosis and SARS-CoV-2 Infection. *Antioxidants*. 2023;12(3):1.
25. Rittirsch D, Huber-Lang MS, Flierl MA, et al. Immunodesign of experimental sepsis by cecal ligation and puncture. *Nat Protoc*. 2009;4(1):31–36. doi:10.1038/nprot.2008.214
26. Matute-Bello G, Downey G, Moore BB, et al. An official American Thoracic Society workshop report: features and measurements of experimental acute lung injury in animals. *Am J Respir Cell Mol Biol*. 2011;44(5):725–738. doi:10.1165/rcmb.2009-0210ST
27. Lee EH, Shin MH, Gi M, et al. Inhibition of pendrin by a small molecule reduces lipopolysaccharide-induced acute lung injury. *Theranostics*. 2020;10(22):9913–9922. doi:10.7150/thno.46417
28. Chen D, Chu B, Yang X, et al. iPLA2β-mediated lipid detoxification controls p53-driven ferroptosis independent of GPX4. *Nat Commun*. 2021;12(1):3644. doi:10.1038/s41467-021-23902-6
29. Gotts JE, Matthay MA. Sepsis: pathophysiology and clinical management. *BMJ*. 2016;353:i1585. doi:10.1136/bmj.i1585
30. Jablonski RP, Kim S-J, Cheresh P, et al. SIRT3 deficiency promotes lung fibrosis by augmenting alveolar epithelial cell mitochondrial DNA damage and apoptosis. *FASEB j*. 2017;31(6):2520–2532. doi:10.1096/fj.201601077R
31. Kurundkar D, Kurundkar AR, Bone NB, et al. SIRT3 diminishes inflammation and mitigates endotoxin-induced acute lung injury. *JCI Insight*. 2019;4(1). doi:10.1172/jci.insight.120722
32. Dikalova AE, Pandey A, Xiao L, et al. Mitochondrial deacetylase sirt3 reduces vascular dysfunction and hypertension while sirt3 depletion in essential hypertension is linked to vascular inflammation and oxidative stress. *Circ Res*. 2020;126(4):439–452. doi:10.1161/CIRCRESAHA.119.315767
33. Zhai M, Li B, Duan W, et al. Melatonin ameliorates myocardial ischemia reperfusion injury through SIRT 3-dependent regulation of oxidative stress and apoptosis. *J Pineal Res*. 2017;63(2). doi:10.1111/jpi.12419
34. Zhang J, Xiang H, Liu J, et al. Mitochondrial Sirtuin 3: new emerging biological function and therapeutic target. *Theranostics*. 2020;10(18):8315–8342. doi:10.7150/thno.45922
35. Su H, Cantrell AC, Chen J-X, et al. SIRT3 deficiency enhances ferroptosis and promotes cardiac fibrosis via p53 acetylation. *Cells*. 2023;12(10):1428. doi:10.3390/cells12101428

36. Sun M, Li J, Mao L, et al. p53 deacetylation alleviates sepsis-induced acute kidney injury by promoting autophagy. *Front Immunol*. 2021;12:685523. doi:10.3389/fimmu.2021.685523
37. Luo J, Su F, Chen D, et al. Deacetylation of p53 modulates its effect on cell growth and apoptosis. *Nature*. 2000;408(6810):377–381. doi:10.1038/35042612
38. Stafford DW. The vitamin K cycle. *J Thromb Haemost*. 2005;3(8):1873–1878. doi:10.1111/j.1538-7836.2005.01419.x
39. Zhang J, Zhu Q, Peng Z, et al. Menaquinone-4 attenuates ferroptosis by upregulating DHODH through activation of SIRT1 after subarachnoid hemorrhage. *Free Radic Biol Med*. 2024;210:416–429. doi:10.1016/j.freeradbiomed.2023.11.031
40. Vervoort LM, Ronden JE, Thijssen HH. The potent antioxidant activity of the vitamin K cycle in microsomal lipid peroxidation. *Biochem Pharmacol*. 1997;54(8):871–876. doi:10.1016/S0006-2952(97)00254-2
41. Liao W, Zhang R, Chen G, et al. Berberine synergises with ferroptosis inducer sensitizing NSCLC to ferroptosis in p53-dependent SLC7A11-GPX4 pathway. *Biomed Pharmacother*. 2024;176:116832. doi:10.1016/j.biopha.2024.116832
42. van der Meer JH, van der Poll T, van 't Veer C. TAM receptors, Gas6, and protein S: roles in inflammation and hemostasis. *Blood*. 2014;123(16):2460–2469. doi:10.1182/blood-2013-09-528752